Combined Analysis of Safety and Optimal Efficacy in UV-light-activated Corneal Collagen Crosslinking

Jui-Teng Lin[1*]

[1]*New Vision Inc, Taipei 103, Taiwan.*

Author's contribution

The sole author designed, analyzed and interpreted and prepared the manuscript.

Original Research Article

ABSTRACT

Aims: To analyze the combined factors for safety and optimal efficacy for UV-light-initiated corneal collagen cross-linking (CXL).
Study Design: Modeling and analysis of CXL.
Place and Duration of Study: New Vision Inc, Taipei, between Oct. 2015 and July 2016.
Methodology: Analytic formulas were derived based on the coupled dynamic equations for the safety dose (E^*), minimum corneal thickness and concentration of the riboflavin, and the cornea stiffness increase after the CXL. The critical parameters influencing the efficacy of CXL include: various absorption coefficients, initial concentration (C_0) and diffusion depth (D) of the riboflavin solution, the quantum yield, the UV light intensity (I_0) and dose (E), irradiation duration (t), the cytotoxic threshold dose of endothelial cells(E') and the corneal thickness (z).
Conclusion: The safety dose (E^*) is an increasing function of the parameter set (D, z, C_0) and has a range of 5.3 to 10.1 J/cm^2 for cytotoxicity threshold 0.63 to 1.26 J/cm^2. Minimum corneal thickness z^* =(300, 400) um for dose of E^*=(5.0, 10.1) J/cm^2 which has a much wider range than the conventional safety dose 5.4 J/cm^2 (with z^*=400 um). For maximum efficacy, the optimal dose is 0.7 to 1.55 J/cm^2. However, to achieve crosslink depth of 230 to 300 um, higher dose of 2.0 to 3.0 J/cm^2 is recommended.

_____

*Corresponding author: E-mail: jtlin55@gmail.com;

1. INTRODUCTION

Photopolymerization has been widely used in many applications ranging from chemical engineering to biomedical engineering and biomaterials [1-4]. It has been used for production of catheters, hearing aids, surgical masks, medical filters, and blood analysis sensors [2]. Photopolymers have also been explored for uses in dentistry, drug delivery, tissue engineering and cell encapsulation systems [3]. Both ultraviolet, visible and infrared lights (360 to 1000 nm) have been used as the photoinitiators for various photosensitizers [3,4].

For ophthalmology applications, corneal collagen cross-linking (CXL) systems have been commercialized for years for human clinical uses [5-10]. Photochemical kinetics of CXL and the biomechanical properties of corneal tissue after CXL are reported [11,12]. However, much less efforts have been invested in basic theoretical studies of photopolymerization [13-21], where Lin et al presented the first dynamic modeling for the safety of CXL[17,18]. The safety and efficacy issues of CXL have been explored clinically and theoretically [10,19-27]. To increase the speed of CXL procedure, they accelerated CXL using high UV power (9 to 45 mW/cm^2) [28-34]. In addition, pulsed mode of the UV light was proposed for potential improvement on CXL efficacy [35,36] as well as femtosecond-laser-assisted pocket was proposed [37]. More recently, a corneal topography-guided CXL was commercialized by Avedro based on a pending US patent[38]. The safety of CXL would be significantly improved if the epithelium could be left in situ. Several methods have been reported for this purpose including the use of benzalkonium chloride EDTA, gentamicin, iontophoresis, as well as minimal trauma (through epithelial poke marks) to the epithelium[10]. A sufficient concentration of riboflavin is pre-required and can be achieved by several methods[5] including: diffusion in the de-epithelialized stroma (standard method); diffusion through the epithelium into the stroma (transepithelial method); or direct introduction of riboflavin into the stroma (pocket technique, ring technique, needle technique); and enrichment of riboflavin in the stroma by iontophoresis [39].

In CXL, both type-I and type-II photochemical reactions occur [11], The photosensitizer riboflavin absorbs the UV energy and is excited to its triplet state (3Rf*). In type-I mechanism, the excited triplet state reacts directly with the collagen proteins and creating substrate free radicals or radical ions of superoxide anion (O_2^-) and OH, respectively, by hydrogen atoms or electron transfer and the sensitizer is consumed during the reaction. In type-II mechanism, the excited sensitizer reacts with oxygen to form reactive singlet oxygen (RSO),$^1O_2$ and regenerates ground state sensitizer. These RSO then further reacts with the collagen covalent bonds between the collagen molecules and proteoglycans to produce additional cross-linked bonds [11]. Unlike type-I process, type II process does not consume sensitizers during the reaction. but requires oxygen and therefore it is the minor mechanism in most CXL processes. CXL can harden the collagen but also damage viable cells when the UV dose is higher than the damage threshold or when the antioxidant defense system is overwhelmed.

It has been reported that oxygen concentration in the cornea is modulated by UV irradiance and temperature and quickly decreases at the beginning of UV light exposure [11]. The oxygen concentration tends to deplete within about 10-15 seconds for irradiance of 3 mW/cm^2 and within about 3-5 seconds for irradiance of 30 mW/cm^2 [11]. By using pulsed UV light of a specific duty cycle, frequency, and irradiance, input from both Type I and Type II photochemical kinetic mechanisms may be optimized to achieve the greatest amount of photochemical efficiency. The rate of reactions may either be increased or decreased by regulating one of the parameters such as the irradiance, the dose, the on/off duty cycle, riboflavin concentration, soak time, and others [11,34,37].

This study will demonstrate that the conventionally accepted criterion having a safety dose E*=5.4 J/cm^2 and a corneal minimum thickness z*>400 μm is just one of the special case meeting our safety criteria. Without specifying the parameters of riboflavin (RF) concentration and its diffusion depth, the conventional safety criteria (E*, z*) = (5.4 J/cm^2, >400 μm) is meaningless. Furthermore, the safety dose E* is proportional to the cytotoxic threshold of endothelial cells. Therefore, the accurate safety dose relies upon the accurate threshold dose which was estimated (or proposed) to be 0.63 J/cm^2 by prior work based

on the measured animal data [25,26]. Moreover, the conventionally accepted UV light absorption in RF solution [22,23] is based only on its initial (at t=0) intensity and ignoring the RF dynamic depletion causing the steady-state intensity higher than the initial value. Therefore, the prior work [22,24] overestimates the dynamic light intensity.

A recent article of Mooren et al [40] evaluated the cytotoxicity threshold for human endothelium with setting from the endothelial side and concluded a much higher value (at least eight times higher) than that of the previously reported animal models (0.63 J/cm^2) [25,26]. Based on their measured human data, the corresponding safety surface dose (based on our calculation) is as high as 27 J/cm^2. This value is much higher than any of the clinically reported data [21-26]. Therefore further validation of the cytotoxicity threshold for human endothelium is required. Furthermore, it was reported by Lombardo et al. [40] that thin cornea with 325 um thickness after the CXL did not shown endothelium damage under a high dose of 5.4 J/cm^2. These reported data indicated that the conventional safety dose [25,26] 5.4 J/cm^2 and minimum corneal thickness of 400 um are underestimated.

This study will demonstrate the new finding that thin human cornea of 300um (much less than the conventional animal model of 400 um) is stilled allowed in CXL-Lasik process for endothelium threshold dose higher than 1.8 J/cm^2. Our new theory will show that the safety dose (E*) and the corneal safety thickness (z*) cannot be set as a constant as that of conventional protocols. Instead, they are variable functions defined by the combined parameter set. This study will use the currently available (or measured) data in the calculations, whereas the unknown parameters will be treated as free parameters within the clinically recognized ranges. This study will focus on the analytic formulas, whereas numerical results based on computer simulations will be shown else where.

2. MATERIALS AND METHODS

2.1 The Modeling System

As shown in Fig. 1, a corneal model consists of its epithelial layer and the underlying stroma collagen. The UV light is normal incident to the corneal surface. A typical CXL protocol is to administer RF on the corneal surface 5 to 10 times at 2 to 5 minute intervals and wait until the

RF solution diffuses into the top layer at approximately 200 to 300 µm. The CXL procedures could be conduced (as shown by Fig. 1) either with epithelium removed (epi-off) with a 0.1% riboflavin-dextran solution or with epithelium intact (epi-on) with a 0.25% riboflavin aqueous solution. It was known that riboflavin diffusion depth in the epi-on case is normally less than that of epi-off and therefore the epi-on is less efficient [5].
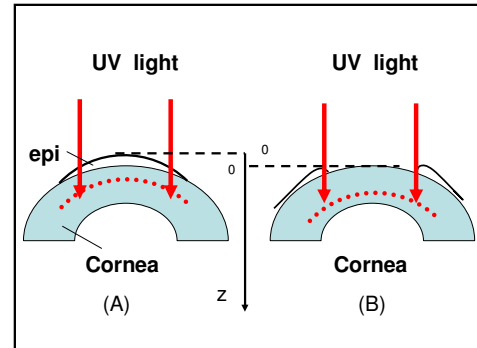

Fig. 1. A corneal model system under UV light cross-linking for the epi-on (A) and epi-off (B) case, where z is along the corneal thickness direction (z=0 for the corneal surface); the red dotted curves define the riboflavin diffusion boundaries [18]

In the above described CXL model, the UV light intensity in the corneal stroma is given by a revised time-dependent Lambert-Beer law [18].

$$I(z,t) = I_0 \exp[-A(t)z] \qquad (1)$$

where the time-dependent extinction coefficient A(t) shows the dynamic feature of the UV light absorption due to the RF concentration depletion. Without the RF, A(t) becomes a constant given by the absorption coefficient of the corneal stroma tissue reported to be[27] A=2.3Q, with Q=13.9 (1/cm). With the RF in the stroma, the initial (at t=0) overall absorption has an extra absorption defined by the extinction coefficient and initial concentration of the RF, i.e. A (t=0) =2.3 (Q $+ \varepsilon_1 C_0$), with the reported data [20,28] $\varepsilon_1 = 204$ (%·cm)$^{-1}$. For t>0, A(t) is an increasing function due to the deletion of C_0 in time and defined by both the extinction coefficient of the RF(ε_1) and its photolysis product (ε_2), where ε_2 is not yet available for human, but was estimated to be about 80 to 120

(%·cm)$^{-1}$, based on measured data in RF solution under UV light irradiation [18].

In the CXL process, the UV light intensity $I(z,t)$ and RF concentration C(z,t) in the corneal stroma may be described by a set of coupled first-order differential equations, or by the integral equations [16-20].

$$I(z,t) = I_0 \exp\left[-2.3\int_0^z \left[(\varepsilon_1 - \varepsilon_2)C(z',t) + \varepsilon_2 C_0 F(z') + Q\right]dz'\right]$$
(2.a)

with the time-dependent RF concentration given by,

$$C(z,t) = C_0 F(z)\exp\left[-aE(z,t)\right]$$
(2.b)

$$E(z,t) = \int_0^t I(z,t')dt'$$
(2.c)

Where $a = 83.6\lambda\phi\varepsilon_1$, with ϕ being the quantum yield and λ being the UV light wavelength; ε_1 and ε_2 are the extinction coefficients of RF and the photolysis product, respectively. I_0 is the initial UV light surface intensity, or $I(z=t=0)=I_0$.; and C_0 is the initial RF surface concentration assuming a distribution profile given by F(z) = 1 − 0.5z/D, or C(z,t=0)=C_0F(z), with a diffusion depth D in the stroma.

The prior work of Schumacher et al[22] based on a non-depleted RF concentration, i.e, the assumption of aE=0 in Eq. (2.b), significantly overestimates the RF concentration for t>0. Moreover, the time-dependent of I(z,t) and C(z,t) in their Eq. (5) and (6) is the pre-treatment time, rather than the actual UV light exposure time. That is, after the pre-treatment time (t'), they treated the CXL as a steady process without solving the dynamics of CXL. Their t' corresponding to our initial time (t=0). The profiles shown in their Fig. 1 are just the initial (at t=0) profiles of our Eq. (2). The prior work of Schumacher et al[22] also used an oversimplified model to assume ε_2 =0. Therefore, their calculated profiles, Fig. 3 and 4, significantly deviate from our exact numerical profiles to be shown later.

The reported measurements [27,28] provide the parameters of ε_1 = 204 (%·cm)$^{-1}$ and Q = 13.9 (cm^{-1}), whereas ε_2 is not yet available in human,

but was estimated to be in the range of 80 to 120 (%·cm)$^{-1}$ by the RF depletion test [17,18] and the quantum yield ϕ will be a free parameter In Eq. (2), the following units are used: C(z,t) in weight percent (%), I(z,t) in (mW/cm^2), λ in cm, Q in (cm)$^{-1}$ and ε_j (for j=1,2) in (%·cm)$^{-1}$. As shown by Eq. (2) that there are three major UV absorption components in the CXL process: the absorption of the stroma tissue (Q), which is independent to the RF concentration; the absorption of the unreacted RF solution (ε_1 C_0), and the photolysis product (ε_2 C_0), both are proportional to the initial RF concentration C_0.

The initial UV light intensity (at t=0) is obtained by the integration of Eq. (2.a) with C(z,0) = C_0 F(z) [18,20].

$$I_1(z,0) = I_0 \exp\left(-A_1 z\right)$$
(3.a)

and the steady state light intensity is derived by using $C(z, t = \infty) = 0$ in Eq. (2.a),

$$I_2(z,\infty) = I_0 \exp\left(-A_2 z\right)$$
(3.b)

where (for j=1,2)

$$A_j = 2.3[Q + \varepsilon_j C_0 G(z)]$$
(3.c)

$$G(z) = [1 - 0.25z / D]$$
(3.d)

where A_1 (for j=1) is the initial state (at t=0) absorption coefficient, independent to ε_2 ; and A_2 (for j=2) is the steady-state absorption coefficient, which is independent to ε_1 because of the complete concentration depletion, $C(z, t = \infty) = 0$. We note that G(z) in Eq. (3.d) is the integration of F(z) over z.

2.2 The Effective and Safety Dose

The effective dose (or fluence) applied to the cornea collagen (at a depth z) for a UV exposure time (t) is defined by [20].

$$E(z,t) = \int_0^t I(z,t')dt'$$
(4)

The UV light intensity is a dynamic function of time and z and requires a full numerical

4

simulation of Eq. (2). For comprehensive analytic formulas, various numerically fit techniques were presented earlier[18-20]. In this study we will use the linear approximation of the light intensity I (z,t) given by the mean value of the initial (I_1) and steady intensity (I_2) defined by $I(z,t) = 0.5[I_1(z) + I_2(z)]$ for t<T and $I(z) = I_2(z) + 0.5[I_1(z) - I_2(z)]$ for steady-state, or t>T, where T is the steady-state cross-linking time given by T=m/(aI_0), with m =12 fit numerically with the exact solution of Eq. (2) to be shown else where.

Time integration of the light intensity, the effective dose (at z) Eq. (4) becomes [20].

$$Eeff(z) = E\exp(-A_2 z) - g \qquad (5)$$

where E =I_0t is the surface dose (at z=0), and g is a correction factor for the transient state given by g= 0.5(I_2 – I_1)(T/E),T=m/(aI_0), with fit parameter m =12. For ε_1 = 204 (%·cm)$^{-1}$, ε_2 =102 (%·cm)$^{-1}$, Q = 13.9 (cm^{-1}) and C_0= 0.1%, we obtain an approximated value of the correction factor g=0.97[exp(-A_2z) - exp(-A_1z)], which is about 15% correction to the steady-state when E= 3.0 to 4.0 J/cm^2 and at z=400 um.

Given the cytotoxicity threshold dose of the endothelium Eeff=E'(at a depth z), the surface safety dose (defined on the corneal surface z=0) is given by E=E* in Eq. (5) to obtain an E*-formula [20].

$$E* = (E'+g)\exp(A_2 z) \qquad (6)$$

At the referenced point of z=400 µm and quantum yield ϕ =0.1, E*(at the reference point)=E_0=7.62(E'+0.067) for ε_1 = 204 (%·cm)$^{-1}$, ε_2 =102 (%·cm)$^{-1}$ and Q = 13.9 (cm^{-1}) for C_0= 0.1%. . However, for low concentration C_0= 0.02%, E_0=4.18(E'+0.0214).

For a given E' and E_0, the normalized safety dose, E*/E_0 is given as follows.

For C_0= 0.1%,

$$E*/E_0 = 0.131(1+B)\exp(A_2 z) \qquad (7.a)$$

$$B = (g - 0.067)/E' \qquad (7.b)$$

For C_0= 0.02%,

$$E*/E_0 = 0.24(1+B)\exp(A_2 z) \qquad (7.c)$$

$$B = (g - 0.021)/E' \qquad (7.d)$$

Using Eq. (5), we obtain the analytic formula for the RF concentration, from Eq. (2.b).

$$C(z,t) = C_0 F(z)\exp[-aE\exp(-A_2 z) + ag] \qquad (8)$$

Equation (8) provides us the formula for the crosslink time[18,20] defined by when C(z,t=T*)/C_0= 0.018, or $E\exp(-A_2 z) - g = M/a$, with M=4, which leads to the formula for the crosslink time (T*) and crosslink depth (z_1) given by

$$T*(z) = T_0(1 + ag/M)\exp(A_2 z) \qquad (9.a)$$

$$z_1 = [\ln(E/E_0) + ag/M]/A_2 \qquad (9.b)$$

Where T_0 is the surface crosslink time given by T_0=T*(z=0)=1000M/(aI_0), for I_0 in mW/cm^2, and $a = 83.6\lambda\phi\varepsilon_1 = 6.2(\phi/0.1)$, with ϕ being the quantum yield, and E_0 = $I_0 T_0$ =M/a is the surface crosslink dose. For M=4, T_0= (644/I_0) (0.1/ ϕ). For example, for I_0 =10 mW/cm^2, we obtain T_0=64.4 and 32.2 seconds, and surface crosslink dose E_0 0 is 0.644 and 0.322 J/cm^2 for quantum yield ϕ=0.1, and 0.2, respectively.

The safety dose (E*) is defined by the maximum dose (on the cornea surface, z=0) without causing the endothelial cells damage (at a depth of z=400 µm), which is given by the measured dose in the animal model [24-26], 3 mW/cm^{2}x60x30 seconds=5.4 J/cm^2. We will show later that the UV intensity at the endothelial cells (at a depth of z=400 µm) estimated as 0.35 mW/cm^2 and the threshold dose 0.35 mW/cm^{2}x60x30=0.63 J/cm^2 are under estimated based on the simplified model [22] assuming a constant RF concentration, or aE=0 in Eq. (2). For human cornea, the damage threshold dose of the endothelial cells were reported to be much higher than the animal model [41].

2.3 The Minimum Thickness and Concentration

Solving Eq. (7.a) for z=z*, using a mean value of G(z=400 um)=0.8, and B<<1 is neglected, we obtain the safety (or minimum) corneal thickness as follows.

For C_0 =0.1%

$$z^* = [\ln(E^*/E_0) + 2.03]/A_2 \qquad (10.a)$$

At $E^*=E_0$ and C_0=0.1%, we obtain z*=400 um, as expected.

Similarly, one may solve Eq. (7.a) for safety (or minimum) concentration

$$C_0^* = [\ln(E^*/E_0) + 2.03 - 32z]/(235Gz) \quad (10.b)$$

For C_0 =0.02%, we solve Eq. (7.c) to obtain

$$z^* = [\ln(E^*/E_0) + 1.43]/A_2 \qquad (11.a)$$

and the safety (or minimum) concentration

$$C_0^* = [\ln(E^*/E_0) + 1.43 - 32z]/(235Gz) \quad (11.b)$$

2.4 The Efficacy Profiles

The kinetic equation of the rate of polymerization is mainly determined by the rate of reacting monomers given by [6,16,20].

$$\frac{d[M](z,t)}{dt} = R(z,t) = K_0[\phi C(z,t)I(z,t)]^{1/2} \quad (12)$$

Above equation shows that photoinitiation rate (R) is a product of two competing factors, the RF concentration and the laser intensity. Therefore, an optimal value of $\varepsilon_1 C_0 I_0$ is expected for a maximum photoinitiation rate.

Using the UV light intensity defined by the mean value Eq. (3) and C(z,t) given by Eq. (8), we obtain analytic formula for the photoinitiation rate (R).

$$R(z,t) = K_0\sqrt{\phi I_0 C_0 F(z)H(z)}\exp[-0.5aE(z)] \quad (13.a)$$

$$H(z) = 0.5[\exp(-A_1 z) + \exp(-A_2 z)] \qquad (13.b)$$

where H(z) is given by the mean intensity $H(z)=0.5(I_1 + I_2)/I_0$, and E(z) is given by an analytic formula, Eq. (5). Taking $dR(z,t)/dC_0 = 0$, $dR(z,t)/d(I_0) = 0$, we obtain the optimal value $C_0^* \propto 1/(\varepsilon_1 + \varepsilon_2)Gz$, and $I_0^* \propto \exp(A_2 z)/(\varepsilon_1 \phi t)$. Moreover, taking, $dR(z,t)/dz = 0$, we may also find an optimal z*. These optimal features are due to the competing between UV light intensity and RF concentration which have opposite trend.

Integration of Eq. (13) over time (t), and using Eq. (5) for E(z), we obtain the profile (z-dependence) of the increase in corneal stiffness (S').

$$S'(z,t) = \frac{2K_0}{1-g}\sqrt{\frac{C_0 FH}{\phi I_0}}[1 - \exp[-0.5(atI_0)\exp(-A_2 z)] \qquad (14)$$

The efficacy of CXL may be defined by the increase in corneal stiffness (S) after CXL given by the total amount of induced crosslink.

Integration of Eq. (14) over z, and taking averaged over the CXL depth (z), we obtain the normalized increase in stiffness (S).

$$S(z,t)/K_0 = \frac{1}{zK_0}\int_0^z S'(z',t)dz' \qquad (15)$$

2.5 The Scaling Laws

From E. (14), for small (atI_0)<<1, the transient state of S'(z,t) is proportional to (atI_0), we obtain the scaling law

$$S_1' \propto (I_0 t)\sqrt{\phi C_0/I_0} \propto t\sqrt{\phi C_0 I_0} \; . \qquad (16)$$

which shows that the transient state of S' is linearly proportional to the exposure time (t) for a given UV intensity (I_0), and is proportional to the square root of I_0 for a given t. However, the steady-state, when (atI_0)>>1, exp(-0.5atI_0)=0 in Eq. (15), has a different scaling law given by

$$S' \propto \sqrt{C_0/(\phi I_0)} \qquad (17)$$

The above steady state is proportional to $I_0^{-0.5}$, comparing to the transient state S is proportional

6

to $I_0^{0.5}$. The opposite trend is due to the time integration over time (t) which causes the dependence of S' as $I_0^{-0.5}$. These features will be reconfirmed by our numerical data later.

The above scaling laws based on the approximated Eq. (13) will be used to analyze the exact numerical results be shown elsewhere. The optimal C_0^* and I_0^* and the scaling laws for S(z,t) may be mathematically derived similar to that of S'(z,t). However, analytic formulas are not available.

3. RESULTS AND DISCUSSION

Numerical calculations of the factors influencing the CXL efficacy based on Eq. (2) and (15) will be presented elsewhere. This paper will focus on the results based on the developed analytic equations (6), (7), (10), (11), (14)- (17). The major clinical issues of CXL will also be discussed.

3.1 The Effective Dose

The conventional CXL procedures are based on the Dresden protocol which requires a surface safety dose of 5.4 J/cm^2 and a minimum corneal thickness of 400 μm. During the UV exposure, riboflavin drops were applied every few minutes for saturated riboflavin concentration in the stroma and extra protection of the corneal endothelial cells. However, the effective dose of CXL is reduced by the extra absorption of this surface layer. For maximum efficacy, the wasted-dose can be avoided by washing out the extra surface riboflavin layer after its sufficient diffusion into the stroma and prior to the UV light exposure. For RF surface layer (with thickness d), the energy absorbed the RF layer is given by Eab=E(t1/t)[1-Re], where t1 is the portion of the exposure period (t) having RF layer on the surface and R is calculated from Eq..(5) with Q=0, and a mean value of A=15 C_0, Re=exp(-15dC_0)=(0.86,0.74), for d= (100, 200) um and C_0=0.1%, For example, for t1/t=0.7, the conventional dose 5.4 (J/cm^2) is reduced to an effective dose of Eeff=E-Eab=4.4 and 4.9 J/cm^2, for d=200 and 100 um. that is 10 % to 20% of the dose, or 5.4 to 1.08(J/cm^2) dose is wasted in the B2 surface layer having a thickness of 100 to 200 um um and concentration of 0.1%. In the current Dresden protocol (using a 5.4 dose J/cm^2), we estimate the effective dose has a range of 4.0 to 5.0 J/cm^2, depending on the frequency of RF instillation during the UV exposure.

The simplified modeling of prior art [22] assuming a constant RF concentration, using A=51 (1/cm) in Eq. (2), overestimates the dynamic light intensity and the effective dose. For example at z=400 um, and E=4.0 J/cm^2, Eq. (5) leads to Eeff= 0.45J/cm^2, with A_2=50.4(1/cm), which is smaller than that of the simplified model 0.52 J/cm^2 based on A_2=51 (1/cm).

3.2 The Safety Dose

As shown by Eq. (6), the safety dose E(z,t) is an exponential increasing function of D, C_0 , ε_2, Q and the corneal thickness (z), as shown by Eq. (7). In a recent article by Mooren et al [40], they evaluated the cytotoxicity threshold for human endothelium (E') and concluded a much higher value (at least 5.4 J/cm^2) than that of the previously reported animal models (0.63 J/cm^2). Using E'=5.4 J/cm^2 the corresponding safety surface dose, based on Eq. (6), gives 5.4x6.3=27 J/cm^2 for C_0=0.04 %. This value seems to be too high clinically. Therefore, the actual cytotoxic threshold of endothelial cells in human requires further studies.

In the following we will discuss the normalized safety dose defined by E*/ E_0 based on Eq. (7), for the case that cytotoxic threshold of endothelium is known at the referenced point z=400 μm, C_0= 0.1% (or 0.02%) D=500 μm and quantum yield ϕ=0.1, with known parameters of ε_1 = 204 (%·cm)$^{-1}$ and ε_2=102 (%·cm)$^{-1}$ and Q = 13.9 (cm^{-1}). The reference dose in Eq. (7), for high concentration C_0= 0.1%, E*(at reference point)=E_0=7.62(E'+0.067) =5.3 and 10.1 J/cm^2, for threshold dose of the endothelial cells E'=0.63 and 1.26 J/cm^2, respectively. However, for low concentration C_0= 0.02%, E_0=4.18(E'+0.0214) which reduce to 2.72 and 5.36 J/cm^2.

Fig. 2 shows the safety dose (E*) and the normalized dose E*/E_0 for C_0=0.1%, D=500 um quantum yield ϕ =0.1, and various cytotoxic threshold E'= (0.63, 1.26, 1.9) J/cm^2. The left figure shows E* is an increasing function of E' (and E_0), whereas the normalized dose is almost independent to the E', that is the 3 curves of the left figure converged to one "universal" curve shown in the right figure. This universal feature may be seen by Eq. (7.a), in which the contribution from B is very small such that E*/E_0 is almost independent to E'. As shown by Fig. 2, for a corneal thickness of 400 um and C_0=0.1%,

D=500 um, the safety dose has a range of 5.3 to 10.1 J/cm^2 depending on the cytotoxicity threshold range of 0.63 to 1.26 J/cm^2. The safety dose based on our theory is much higher than the conventionally quoted value of 5.4 J/cm^2 based on animal model having E'=0.63 J/cm^2. Fig. 2 shows that for E*=(0.65, 1.0, 1.3)E$_0$, the minimum corneal thickness is z* =(300, 400, 450) um. For examples, for C$_0$=0.1% and D=500 um, E*=10.1J/cm^2 (for E'=0.63 J/cm^2), z*=(300, 400) um, for dose of E*=(5.0, 10.1) J/cm^2.

Fig. 3 shows the normalized safety dose (E*/E$_0$) versus C$_0$ for D=500 µm at various corneal thickness z = (350, 400, 450) um, Fig. 4 shows E*/E$_0$ versus z, for C$_0$ =0.1% at various diffusion depth D= (200, 300, 500) um. These data show that E*/E$_0$ is a nonlinear increasing function of C$_0$, D, and z, as also shown by Eq. (3.c) and (7).

3.3 The Minimum Corneal Thickness

Fig. 5 shows that for a given safety dose E*=E$_0$, the safety (minimum) corneal thickness (z*) is a decreasing function of the RF concentration but is an increasing function of the diffusion depth D as also shown by Eq. (10). For C$_0$= 0.1%, E$_0$=(5.3,10.1, 15) J/cm^2, for cytotoxicity threshold E'=(0.63, 1.26, 1.9) J/cm^2. Therefore z*= (400, 425) um, for D=(500, 300) um and E*=5.3 J/cm^2 (for E'=0.63 J/cm^2), or E*=10.1 J/cm^2 (for E'=1.26 J/cm^2), Therefore the conventional dose 5.4 J/cm^2 is safe for a corneal thickness of 400 um, but requires D>500 um and C$_0$= 0.1% when E'=0.63 J/cm^2. However, if E'=1.26 J/cm^2, then the safety dose is much higher, E*=10.1 J/cm^2.
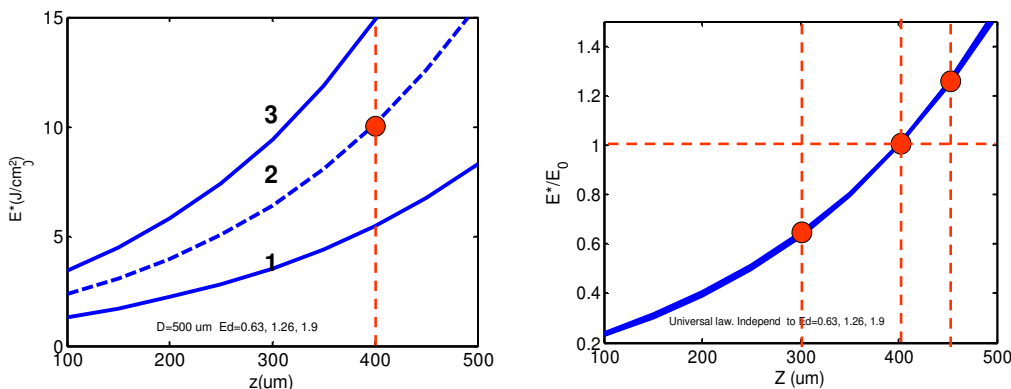

Fig. 2. The safety dose (E*, left figure) and normalized safety dose (E*/E$_0$, in right figure) versus z for C$_0$=0.1%, D=500 um, quantum yield ϕ=0.1 and E'= (0.63, 1.26, 1.9) J/cm^2, for curves (1,2,3) in left figure, where the red dot (in left figure) represents E*=E$_0$ at the reference point (z=400 um and E'=1.26 J/cm^2)
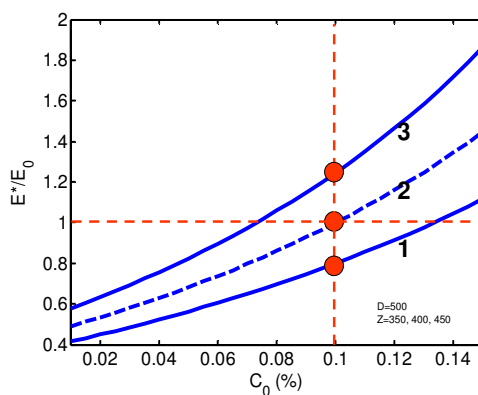

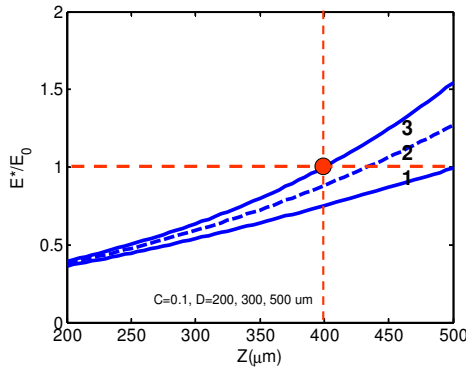**Fig. 3. The normalized safety dose (E*/E$_0$) versus C$_0$ for D=500 µm and z = (350, 400, 450) µm, for curve (1,2,3)**

8

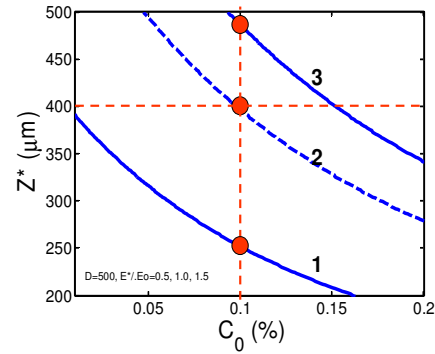**Fig. 4. The normalized safety dose (E*/E$_0$) versus z, for C$_0$ =0.1% and D= (200, 300, 500) μm, for curve (1,2,3)**

Fig. 6 shows z* versus C$_0$ for D=500 um showing that z* is an increasing function E*/ E$_0$. These calculated data show that small D and C$_0$ require large corneal thickness to protect the endothelium cells. As shown by Fig. 6, the safety corneal thickness z*=(250, 400, 490) um, for E*/E$_0$= (0.5, 1.0, 1.5). Therefore the conventional dose E*=5.4 J/cm^2 is safe even in thin corneas of 250 um if E$_0$ = 10.8 J/cm^2 or when E'=1.35 J/cm^2, calculated from E$_0$=7.62(E'+0.069), when C$_0$= 0.1% and D=500 um.

The above examples demonstrate that thin human cornea of 300 um (much less than the conventional animal model of 400 um) is stilled allowed in CXL-Lasik process as far as the endothelium threshold dose is higher than 1.26 J/cm^2 which was reported recently [40,41].
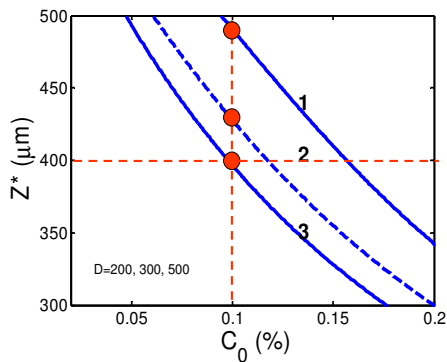

Fig. 5. The safety corneal thickness (z*) versus concentration for E*/E$_0$=1.0 and D =(200, 300, 500) um for curve (1,2,3)

Fig. 6. Same as Fig. 5, but for D=500 um and E*/E$_0$ =(0.5, 1.0, 1.5) for curve (1,2,3)

3.4 The Stiffness Profiles and Crosslink Depth

Detailed computer simulations for the influence of each of the parameters of [C$_0$, D, I$_0$, t, ϕ] in the increase of stiffness defined by Eq. (14) and (15) will be shown elsewhere. This paper is focusing on the features summarized from the numerical simulations, besides typical examples of the stiffness profiles. Fig. 7 shows the typical profiles (z-dependence) of the increase in corneal stiffness (S') for a fixed UV light intensity I$_0$=10 W/cm^2, defined by Eq. (14). Each profile has a maximum value S* (at the crosslink depth Z*), where both S* and Z* are increasing function of the UV exposure time (t), or dose (for a given light intensity). We note that the crosslink depth (Z*) calculated numerically by the maximum S* has the similar functional form as that of Eq. (9.b) which is analytically derived.

Fig. 8 shows S' versus z for a fixed exposure time t=100 s, but for various UV light intensity, where S* is a decreasing function of the UV light intensity (for a given exposure time), whereas Z* is an increasing function of I$_0$ (or dose E$_0$=tI$_0$) which is shown in Fig. 9 and can be well fit by Eq. (9.b) with ag/M=0.07. By more simulation profiles for various D and C$_0$ (not shown here), we found Z* versus C$_0$ and D in Fig.10 and 11. Combining the curves shown by Figs. 9 to 11, we are able to figure out the following approximate analytic equations for S* and Z* for the linear regime (for dose between 2.0 and 3.0 J/cm^2 as shown in Fig. 8).

$$S^* = 10 - 0.5(E-2.0) + 62(C_0 - 0.1) + 0.005(D-500)$$
(18.a)

$$Z^* = 229 + 71(E-2.0) - 880(C_0 - 0.1) + 0.21(D-500)$$
(18.b)

where units are S^* in K_0, E in J/cm^2, C_0 in %, Z^* and D in um. Eq. (18) provides the important feature that S^* is an increasing function of C_0 and D, but it is a decrease function of E. In comparison, Z^* is an increasing function of E and D, but it is a decrease function of C_0.
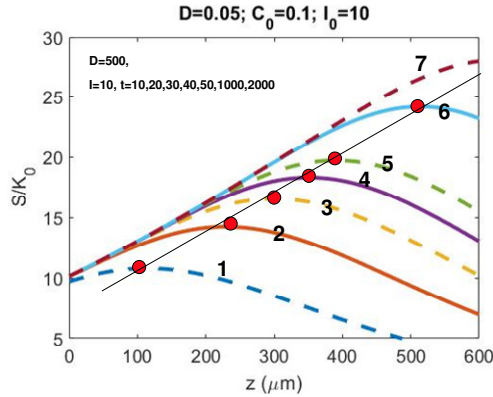

Fig. 7. The profile (z-dependence) of the increase in corneal stiffness (S') for C_0= 0.1%, D=500um, quantum yield ϕ=0.1 and fixed UV light intensity I_0=10 W/cm^2 for various exposure time t=(10, 20, 30,40,50, 100, 200) s, shown by curves (1,2,3,4,5,6,7)

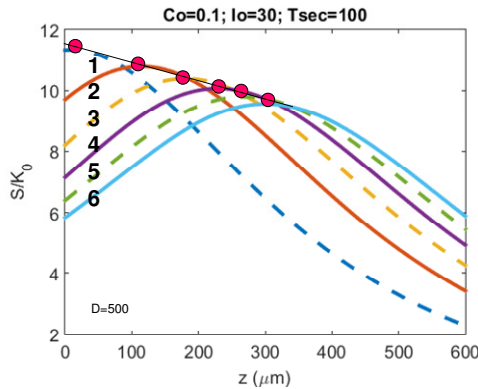**Fig. 8. Same as Fig. 7 but for a fixed exposure time t=100 s, and various UV light intensity I_0= (5,10,15,20,25,30) mW/cm^2 shown by curves (1,2,3,4,5,6,7)**

3.5 The Optimal Efficacy

CXL efficacy may be described by the normalized increase in stiffness (S/K_0) as shown by Eq. (15). Numerical simulations (to be presented elsewhere) shows S/K_0 versus dose

(E_0) for C_0 = (0.05, 0.1)% and D=(200, 300, 500) um, where optimal dose of E_0^*=(0.7, 1.3, 1.55) J/cm^2 for D=(200, 300, 500) um and C_0 = 0.1%. The increase in stiffness (S/K_0) decreases about 10% to 18% from the maximum values for dose of 2.0 to 3.0 J/cm^2 which are higher than the optimal value of 0.7 to 1.55 J/cm^2.

As shown in Fig. 9, the crosslink depth is only Z^*=(120 to 170) um at the optimal dose E_0^*=(0.7 to 1.3) J/cm^2. To achieve Z^* in the range of 230 to 300 um (as shown by Fig. 9), one requires higher dose of E_0=2.0 to 3.0 J/cm^2 despite the drop of 10% to 18% from its optimal value.

Numerical simulations to confirm the scaling laws shown by Eq. (16) will be presented elsewhere.
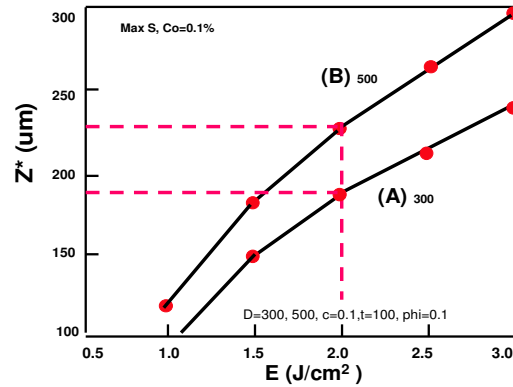

Fig. 9. Crosslink depth (Z^*) versus UV light dose (E) for D=300 um (curve (A) and D=500 um (curve (B) for C_0= 0.1% and a fixed exposure time t=100s, for various UV light intensity I_0= 5 to 30 mW/cm^2, or dose E=0.5 to 3.0 J/cm^2
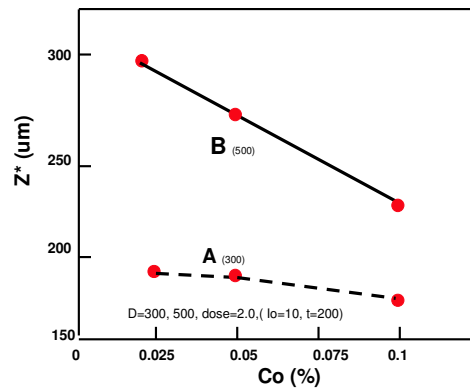

Fig. 10. Same as Fig. 9 but for Z^* versus C_0 for UV light intensity of I_0= 10 mW/cm^2, and exposure time t=200s (or dose of 2.0 J/cm^2)
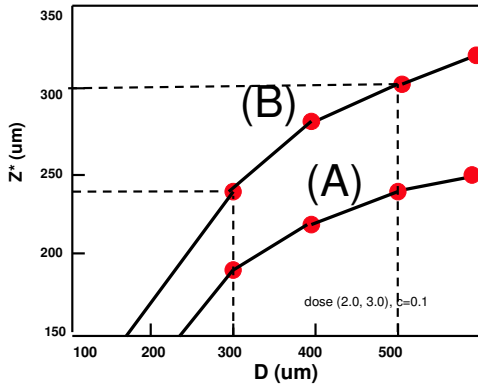
Fig. 11. Cross linking depth (Z*) versus diffusion depth (D) for dose of 2.0 J/cm^2, curve (A) and 3.0 J/cm^2, curve (B), C$_0$=0.1% and quantum yield ϕ=0.1

3.6 The clinical issues

3.6.1 The effective dose

As shown by Eq. (5), the effective dose is given by the parameters of the three UV absorption coefficients [$\varepsilon_1, \varepsilon_2$, Q], the quantum yield (ϕ), the RF concentration (C$_0$), and diffusion depth (D) and the corneal thickness(z), where the values of ε_1 and Q have been measured [27,28]. However, ε_2 and Q are not yet available and treated as free parameters in our calculations. In epi-on situation, typical value of C$_0$=0.1% is used and Eq. (5) allows us to predict the effective dose

when ε_2 and Q are available in the future. Using a reasonable value of ε_2 =102(%·cm)$^{-1}$ and Q=13.9 (cm^{-1}), and the conventional dose 5.4 (J/cm^2) in a Dresden protocol is reduced to 4.0 to 5.0 J/cm^2, depending on the frequency of RF instillation during the UV exposure, or the thickness of the RF surface layer (about 100 to 200 um). Therefore for efficient CXL the extra RF layer should be washed out prior to the UV exposure. We note that a wide range of the peak RF concentration (C$_0$) were reported 0.04% [40], 0.06% [41], 0.02% [42] and 0.1% [22], therefore further clinical measurements are needed for conclusive values.

3.6.2 The safety dose

The cytotoxicity threshold endothelium cells (E') was reported in an animal model of 0.63 J/cm^2. [26] which is much lower than the reported human data [40] of at least 5.4 J/cm^2. The corresponding safety surface dose (at the reference point of z=400 um and C$_0$=0.1%), based on Eq. (6), is 5.3 J/cm^2 (using animal model) and 27 J/cm^2 using human mode which seems to be too high clinically. Therefore, the actual cytotoxic threshold of endothelial cells in human requires further studies. Knowing the actual value of E', $\varepsilon_1, \varepsilon_2$, Q, ϕ, and the RF concentration(C$_0$), Eq. (6) allows us to predict the accurate safety dose (E*) at a given corneal thickness (z).
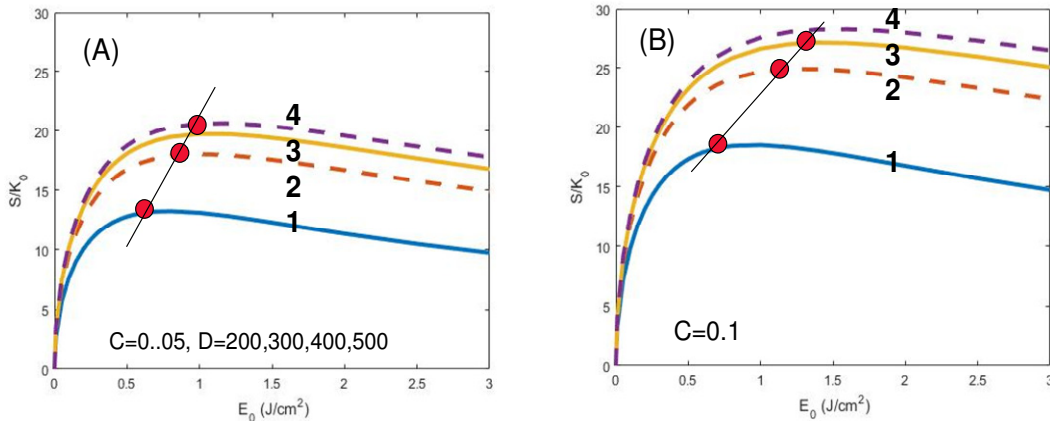

Fig. 12. Normalized maximum stiffness increase (S*/K$_0$) versus dose (E$_0$) for C$_0$ = (0.05, 0.1)% (Fig. A,B) and D=(200, 300, 500) um, for curves (1,2,3,4). The red dots show the optimal dose E$_0$* for various D

3.6.3 The accelerated CXL protocol

The accelerated CXL uses a higher UV intensity (for a fixed dose of 5.4 J/cm^2) to reduce the UV exposure time (t) based on the Bunsen-Roscoe law (BRL) that a photochemical reaction will stay constant if the total energy is constant and a shortened irradiation time at higher irradiance should lead to the same increase in biomechanical stiffness as a longer irradiation time at lower irradiance. For examples: t=(30, 10, 5, 3, 2) minutes, for UV intensity I_0=(3, 9, 18, 30, 45) J/cm^2 based on BRL. This linear feature may be described by Eq. (9), where the surface crosslinking time given by $T_0=T^*(z=0)=1000M/(aI_0)$ which follows the RBL. However the T^* (with z>0) is a nonlinear function of I_0 and does not follow the RBL to be further analyzed as follows.

3.6.4 The nonlinear scaling laws

As shown by Eq. (16.b), the scaling laws predict the nonlinear features against the RB law which was also reported clinically [29]. Eq. (16.b), also shown by Fig. 8, predicts the steady state maximum stiffness (or efficacy) is proportional to $I_0^{-0.5}$, that is the UV exposure time (for a given dose) should be adjusted for longer than those based on the linear RBL.

3.6.5 The optimal dose

As shown by Fig. 9 and 12, to achieve Z^* in the range of 220 to 300 um, one requires a dose of E_0=2.0 to 3.0 J/cm^2 which is much lower than the conventional "appearance" dose of 5.4 J/cm^2, but slightly lower than the effective dose of 4.4 to 4.9 J/cm^2. (after reducing the absorption of the RF surface layer).

3.6.6 The role of concentration and diffusion depth

As show by Eq. (17), and Fig.10, the crosslink depth (Z^*) is an increasing function of the diffusion depth (D), but a decreasing function of the concentration (C_0). Therefore, installation of the RF solution on the epi-off corneal surface must be long enough (at least 15 minutes) to allow a deep diffusion depth D>500 um. Furthermore, while higher concentration achieves larger peak stiffness, it also suffers a smaller crosslink depth, as shown by Eq. (17) and Fig. 10. Therefore optimal concentration range of 0.8% to 1.2% are recommended. It should be noted that the RF solution concentration is always less than the effective concentration diffused into the stroma per reported data. [40-42].

4. CONCLUSION

We have presented, for the first time, analytic formulas for the safety dose, minimum corneal thickness and RF concentration characterized by the extinction coefficient (A), concentration and the diffusion depth of the riboflavin, the UV light intensity, dose, irradiation duration (t), and the corneal thickness (z). The safety dose (E^*) is an increasing function of the parameter set (D, z, C_0) and has a range of 5.3 to 10.1 J/cm^2 for cytotoxicity threshold 0.63 to 1.26 J/cm^2. Minimum corneal thickness z^* =(300, 400) um for safety dose of E^*=(5.0, 10.1) J/cm^2 which is much higher than the conventional dose 5.4 J/cm^2 (with z^*=400 um). For maximum efficacy, the optimal dose is 0.7 to 1.5 J/cm^2. However, to achieve crosslink depth of 230 to 300 um, higher dose of 2.0 to 3.0 J/cm^2 is recommended. It should be noted that the formulas presented in this study would require further justification by clinical data (for human corneas), particularly the measured value of the extinction coefficients of the photolysis product, the quantum yield and the cytotoxic threshold of the endothelium cells which are not yet available.

CONSENT

It is not applicable.

ETHICAL APPROVAL

It is not applicable.

ACKNOWLEDGEMENTS

COMPETING INTERESTS

The author is the CEO of New Vision Inc. and has financial interest.

REFERENCES

1.   Odian G. Principles of polymerization. New York: Wiley; 1991.

2.   Ravve A. Light-Associated reactions of synthetic polymers. New York: Spring Street; 2006.

3.   Reichmanis E, Crivello J. Photopolymer materials and processes for advanced technologies. Chem. Mater. 2014;26:533–548.

4.   Fouassier JP, Allonas X, Burget D. Photopolyermziation reactions under visible lights: Principle, mechanisms and examples of applications. Progress in Organic Coatings. 2013;47:16–36.

5.   Hafezi F and Randleman JB. Editors. corneal collagen cross-linking, first ed. Thorofare (NJ): SLACK; 2013.

6.   Sorkin N, Varssano D. Corneal collagen cross-linking: A systematic review. Ophthalmologica. 2014;232:10-27.

7.   Li N, Peng XJ, Fan ZJ. Progress of corneal collagen cross-linking combined with refractive surgery. Int J Ophthalmol. 2014;7:157-162.

8.   Khandelwal SS, Randleman JB. Current and future applications of corneal cross-linking. Curr Opin Ophthalmol. 2015;26(3):206-213.

9.   Kymionis GD, et al. Corneal collagen cross-linking (CXL) combined with refractive procedures for the treatment of corneal ectatic disorders: CXL plus. J Refract Surg. 2014;30:566-576.

10. Shalchi Z, Wang X, Nanavaty MA. Safety and efficacy of epithelium removal and transepithelial corneal collagen cross-linking for keratoconus. Eye. 2015; 29:25-29.

11. Kamaev P, Friedman MD, Sherr E, Muller D. Cornea photochemical kinetics of corneal cross-linking with riboflavin. Vis. Sci. 2012;53:2360-2367.

12. Beshtawi IM, et al. Biomechanical properties of corneal tissue after ultraviolet-A-riboflavin cross-linking. J Cataract Refract Surg. 2013;39(3):451-462.

13. Miller GA, Gou L, Narayanan V, Scranton AB. Modeling of photobleaching for the photoinitiation of thick polymerization systems. J Polym Sci A1. 2002;40:793-808.

14. Terrones G, Pearlstein AJ. Effects of optical attenuation and consumption of a photobleaching initiator on local initiation rates in photopolymerizations. Macromolecules. 2001;34:3195-32044.

15. Lin JT, Liu HW, Cheng DC. Modeling the kinetics of enhanced photo-polymerization by a collimated and a reflecting focused UV laser. Polymers. 2014;6:1489-1501. DOI:10.3390/polym6051489.

16. Lin JT, Cheng DC. Optimal focusing and scaling law for uniform photo-polymerization in a thick medium using a focused UV Laser, Polymers. 2014;6:552-564.

17. Lin JT, Liu HW, Cheng DC. On the dynamic of UV-Light initiated corneal cross-linking. J. Med Biolog Eng. 2014;34:247-250. DOI: 10.5405/jmbe.15332.

18. Lin JT, Cheng DC, Chang C, Yong Zhang. The new protocol and dynamic safety of UV-light activated corneal collagen cross-linking. Chinese J Optom Ophthalmol Vis Sci. 2015;17:140-147.

19. Lin JT, Wang KC. Analytic formulas and numerical simulations for the dynamics of thick and non-uniform polymerization by a UV light. J Polymer Research. 2016; 23:53-59.

20. Lin JT. Analytic formulas for the clinical issues of a UV-light-activated corneal cross-linking device. J Biomed Eng Devic. 2016;1:104. doi:10.4172/jbemd.1000104.

21. Lin JT. Analytic formulas on factors determining the safety and efficacy in UV-light sensitized corneal cross-linking. Invest Ophthalmol Vis Sci. 2015;56:5740-574.

22. Schumacher S, Mrochen M, Wernli J, Bueeler M, Seiler T. Optimization model for UV-riboflavin corneal cross-linking. Invest Opthamol Vis Sci. 2012;53:762-769.

23. Søndergaard AP, Hjortdal J, Breitenbach T, Ivarsen A. Corneal distribution of riboflavin prior to collagen cross-linking. Curr Eye Res. 2010;35:116-121.

24. Spoerl E, Mrochen M, Sliney D, Trokel S, Seiler T. Safety of UVA-riboflavin cross-linking of the cornea. Cornea. 2007;26:385–389.

25. Spoerl E, Hoyer A, Pillunat LE, Raiskup. Corneal cross-linking and safety issues. Open Ophthalmol J. 2011;5:14–16.

26. Wollensak G, Spoerl E, Wilsch M, Seiler T. Endothelial cell damage after riboflavin–ultraviolet-A treatment in the rabbit. J Cataract Refract Surg. 2003;29:1786–90.

27. Koppen C, Gobin L, Tassignon MJ. The absorption characteristics of the human cornea in ultraviolet-a cross-linking. Eye Contact Lens. 2010;36:77-80.

28. Schumacher S, Mrochen M, Spoerl E. Absorption of UV-light by riboflavin solutions with different concentration. J Refract Surg. 2012;28:91-92.

29. Wernli J, Schumacher S, Spoer E, Mrochen M. The efficacy of corneal cross-linking shows a sudden decrease with very high intensity UV light and short treatment time. Invest. Ophthalmol Vis Sci. 2013;54:1176-1180.

30. Lanchares E del Buey MA Cristóbal JA Lavilla L Calvo B. Biomechanical property analysis after corneal collagen cross-linking in relation to ultraviolet A irradiation time. Graefes Arch Clin Exp Ophthalmol. 2011;249:1223–1227.

31. Mita M, Waring GO, Tomita M. High-irradiance accelerated collagen cross-linking for the treatment of keratoconus: Six-month results. J Cataract and Refract Surg. 2014;40:1032-1040.

32. Richoz O, Kling S, Hoogewoud F, et al. Antibacterial efficacy of accelerated photoactivated chromophore for keratitis-corneal collagen cross-linking (PACK-CXL). J Cataract and Refract Surg. 2014;30:850-854.

33. Mrochen M. Current status of accelerated corneal cross-linking. Indian journal of ophthalmology. 2013;61:428-429.

34. Cinar Y, Cingu AK, Turkcu FM, et al. Comparison of accelerated and conventional corneal collagen cross-linking for progressive keratoconus. Cutaneous and ocular toxicology. 2014;33:218-222.

35. Mazzotta C, Traversi C, Caragiuli S, Rechichi M. Pulsed vs continuous light accelerated corneal collagen cross-linking: in vivo qualitative investigation by confocal microscopy and corneal OCT. Eye. 2014;28:1179-1183.
DOI:10.1038/eye.2014.163.

36. Freidman MD, et al. Systems and methods for corneal cross-linking with pulsed light. US Patent Publication number WO2014014521 A1; 2014.

37. Balidis M, Konidaris VE, Ioannidis G, Kanellopoulos AJ, Femtosecond-assisted intrastromal corneal cross-linking for early and moderate keratoconus. Eye. 2015;28: 1258-1260.
DOI:10.1038/eye.2014.155.

38. Muller D, et al. Controlled cross-linking initiation and corneal topography feedback systems for directing cross-linking. US Patent Publication number EP2712311A1; 2014.

39. Bikbova G1, Bikbov M. Transepithelial corneal collagen cross-linking by iontophoresis of riboflavin. Acta Ophthalmol. 2014;92:30-4.
DOI: 10.1111/aos. 122335.

40. Mooren P, Gobin L, Bostan N, et al. Evaluation of UVA cytotoxicity for human endothelium in an ex vivo corneal cross-linking experimental setting. J Refract Surg. 2016;32:4-46.

41. Lombardo G, Micali NL, Villari V, et al. All-optical method to assess stromal concentration of riboflavin in conventional and accelerated UV-A irradiation of the human Cornea. Invest Opthamol Vis Sci. 2016;57:476-483.
DOI:10.1167/iovs.15-18651.

42. Laggner M, Pollreisz A, Schmidinger G, et al. Correlation between multimodal microscopy, tissue morphology, and enzymatic resistance in riboflavin-UVA cross-linked human corneas. Invest Ophthalmol Vis Sci. 2015;56:3584–35922.